Synthesis, Characterization, and Bioconjugation of Fluorescent Gold Nanoclusters toward Biological Labeling Applications

Cheng-An J. Lin,[†,¶] Ting-Ya Yang,[†,¶] Chih-Hsien Lee,[†,¶] Sherry H. Huang,[†,¶] Ralph A. Sperling,[‡] Marco Zanella,[‡] Jimmy K. Li,[†,¶,#] Ji-Lin Shen,[§] Hsueh-Hsiao Wang,[⊥] Hung-I Yeh,[⊥] Wolfgang J. Parak,[‡,*] and Walter H. Chang[†,¶,*]

[†]Department of Biomedical Engineering, Chung Yuan Christian University, Chung-Li 32023, Taiwan, ROC, [‡]Fachbereich Physik, Philipps Universität Marburg, Renthof 7, 35037 Marburg, Germany, [§]Department of Physics, Chung Yuan Christian University, Chung-Li 32023, Taiwan, ROC, [⊥]Cardiac Medicine, Mackay Memorial Hospital, Taipei, Taiwan, ROC, and [¶]R&D Center for Membrane Technology, Center for Nano Bioengineering, Chung Yuan Christian University, Chung-Li 32023, Taiwan, ROC. [#]Present address: Harvard—MIT Health Sciences and Technology, Brigham and Women's Hospital, Harvard Medical School, Cambridge, Massachusetts 02139.

ABSTRACT Synthesis of ultrasmall water-soluble fluorescent gold nanoclusters is reported. The clusters have a decent quantum yield, high colloidal stability, and can be readily conjugated with biological molecules. Specific staining of cells and nonspecific uptake by living cells is demonstrated.

KEYWORDS: colloidal gold · fluorescent nanoparticles · nanoclusters

Noble metal nanoclusters (NCs) such as Au and Ag with sizes below 2 nm have gained great attention in the past decade. Focus of interest ranges from fundamental properties such as photoluminescence,[1−8] optical chirality,[9−12] ferromagnetism,[13] and redox-like and quantized double layer charging behavior[14−17] to potential applications such as single molecule optoelectronics,[18,19] sensing,[20] and bioassays.[21,22] This is based on the particular size-dependent properties of the clusters. They can be considered as intermediates between atomic and nanoparticle (>2 nm) behavior.[23] Gold nanoparticles (NPs) show a size-dependent plasmon absorption band when their conduction electrons are confined to dimensions smaller than the electron mean free path-length (ca. 20 nm).[24] However, Au nanoparticles smaller than 2 nm (which we term Au nanoclusters) no longer possess plasmon resonance and Mie's theory no longer can be applied.[25−27] In fact small metal NCs have sizes comparable to the Fermi wavelength of electrons (ca. 0.7 nm), which results in molecule-like properties including size-dependent fluorescence[20,23,28] and discrete size-dependent electronic states.[14,29−31] So far there are only few studies about the fluorescence of metal NCs,[32−34] though photoluminescence (PL) of noble metals is a known phenomenon. First reports are based on bulk metals,[35] but soon quasi-size dependence was discovered by the fact that the PL is enhanced on roughened surfaces[36] (i.e., at conditions with reduced radius of curvature).

The fluorescent properties of Au NCs make them potential labels for biologically motivated experiments.[37] Compared to commonly used CdSe/ZnS semiconductor NPs (so-called quantum dots), which possess size-dependent fluorescence in cases where the particle size is smaller than the exciton Bohr radius (about 4−5 nm for CdSe),[38] Au NCs do not contain toxic heavy metals.[39] Though depending on their size also, Au NCs can have cytotoxic effects, for example by binding to DNA[40] they are a potential alternative to quantum dots as fluorescence labels. In this work we describe an easy synthesis for water-soluble fluorescent Au NCs and compare their performance in terms of colloidal and photophysical properties to the one of colloidal CdSe/ZnS NPs. The focus hereby is set on a detailed characterization of practically important parameters rather than on understanding the underlying mechanisms.

RESULTS AND DISCUSSION

Photophysical Characterization. Synthesis of Au NCs was based on precursor-induced Au NP etching in organic phase and ligand

*Address correspondence to whchang@cycu.edu.tw, Wolfgang.Parak@physik.uni-marburg.de.

Received for review September 29, 2008 and accepted December 31, 2008.

Published online January 27, 2009. 10.1021/nn800632j CCC: $40.75

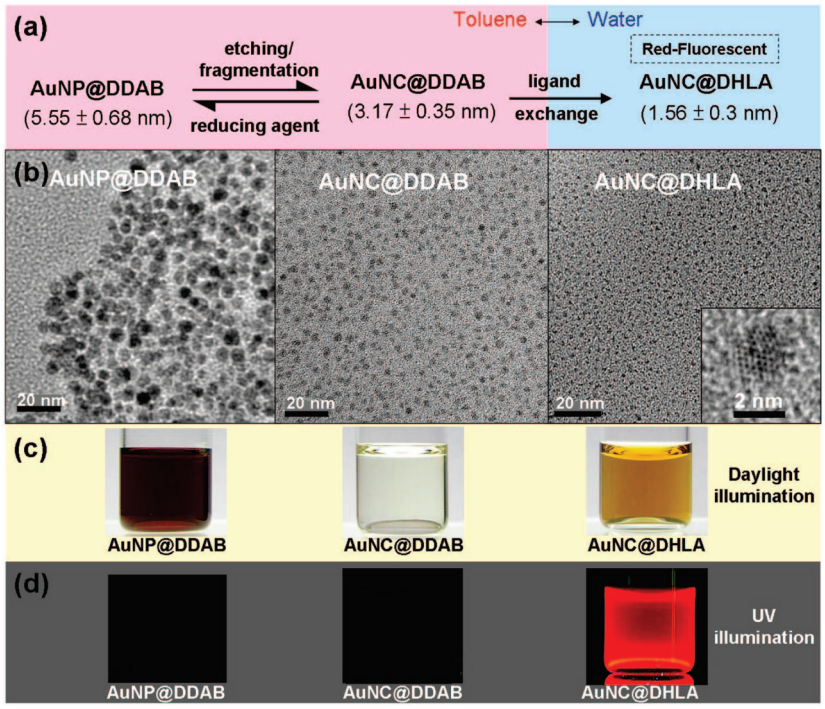

Figure 1. (a) General strategy to fabricate water-soluble fluorescent Au nanoclusters. DDAB-stabilized gold nanoparticles (AuNP@DDAB) are etched by the addition of Au precursors ($HAuCl_4$ or $AuCl_3$) to smaller nanoclusters (AuNC@DDAB). By the addition of reducing agent (TBAB) the Au NCs grow again reversibly into bigger Au NPs. The hydrophobic AuNC@DDAB become water soluble upon ligand exchange with dihydrolipoic acid (AuNC@DHLA); (b) TEM images of AuNP@DDAB, AuNC@DDAB, and AuNC@DHLA; 100 particles were randomly selected for measuring the size distribution, resulting in 5.55 ± 0.68 nm, 3.17 ± 0.35 nm, and 1.56 ± 0.3 nm in diameter, respectively. (c) Pictures of particle solutions under daylight. Contrary to AuNP@DDAB solution which features the red color of surface plasmon absorption, AuNC@DDAB and AuNC@DHLA display a colorless and brown translucent solution without plasmon absorption, respectively. (d) Pictures of the same particle solutions under UV excitation. The AuNC@DHLA solution shows red photoluminescence.

exchange with reduced lipoic acid (DHLA, dihydrolipoic acid) to transfer the particles into aqueous solution. Only after phase transfer to aqueous solution do the NCs exhibit a pronounced red photoluminescence. Exposure of the AuNC@DHLA particle solution to UV light (365 nm) led to an increase in photoluminescence (photobrightening). Photoluminescence (PL) and photoluminescence excitation (PLE) spectra of the cluster solution are shown in Figure 2. The nonshifted emission peak *via* changing the excitation wavelength gives strong evidence that the observed emission is a real luminescence from the relaxed states rather than scattering effects. Using Rhodamine 6G ($Q = 0.95$ in ethanol) as the reference, the quantum yield (Q) of AuNC@DHLA was determined to be 3.45 ± 0.41% in methanol and 1.83 ± 0.32% in water (pH 9). This is 8 orders of magnitude higher with respect to the quantum yield reported for bulk gold ($Q = 10^{-10}$),[35] approximately 1∼2 orders of magnitude higher than the quantum yield of Au NCs derived with other synthesis routes ($Q = 10^{-3} - 10^{-6}$),[1,2,5,30,41,42] and comparable to the quantum yield recently reported by Huang *et al*. for similar Au NCs.[20] Though the quantum yield of the AuNC@DHLA nanoclusters is still 1 order of magnitude lower than that of most organic fluorophores and quantum dots, it is already in the range needed for applications in optical devices and biosensors.

Impurities are always problematic for working with colloidal particles, as they can coexist in the solution so that the optical properties detected from this solution comprise both, the particles and the impurities. As will be explained in the following sections we were able to separate particles from potential impurities such as excess ligands or precursors by size exclusion chromatography and gel electrophoresis, and the presence of the NCs in the purified solutions was verified with TEM. In this way it was assured that the photoluminescence originates from the NCs.

Photoluminescence of Au NCs has been reported before and several models have been proposed to explain this photoluminescence mechanism. Though this study does not contribute in understanding the origin and mechanism of photoluminescence of Au NCs there is work by other groups in this direction. A theoretical study explains photoluminescence of nanosized noble metals by electronic transitions between occupied d bands and states above the Fermi level (usually the sp bands).[29] Whetten *et al*. attribute photoluminescence in the red/near-infrared (NIR) of Au NCs comprising 28 Au atoms capped with glutathione to the recombination between the ground-state and two distinctively different excited states, that is, an intraband and interband transition.[5] Murray *et al*. associated the photoluminescence to interband transitions between the filled $5d^{10}$ band and the $6(sp)^1$ conduction band[2] or to participation of localized core surface states.[43] Other possible mechanisms have been suggested such as ligand-to-metal charge transfer (LMCT) which is mainly affected by the types of ligands,[20] and ligand-to-metal−metal charge transfer (LMMCT) which is commonly referred to as aurophilic interaction.[44] Also fluorescence emission of larger gold nanoparticles has be reported recently.[45]

In an additional experiment photostability of different water-soluble fluorophores was compared (for data see the Supporting Information). The fluorescent gold nanoclusters (AuNC@DHLA) as synthesized here exhibited less photobleaching than organic fluorophores (fluorescein, rhodamine 6G). However, AuNC@DHLA was more prone to photobleaching than semiconductor quantum dots (CdSe/ZnS), which show an excellent photostability.

Colloidal Characterization. To purify the NCs from eventual residual impurities, size exclusion chromatography

and gel electrophoresis was applied. These methods fractionate the initial particle solution and only the desired fraction containing the particles is extracted from the elution profile. As both methods are sensitive to size (gel electrophoresis is in addition sensitive to charge) also estimates of size of the NCs can be extracted from the time-resolved elution profiles.[46] The hydrodynamic diameter d_{eff} of AuNC@DHLA nanoclusters was determined with size exclusion chromatography to be $1.3 < d_{eff} < 3.4$ nm using 1−3 kDa polyethylene glycol (PEG) molecules as size standard[46] (Figure 3a). Similarly the hydrodynamic diameter of AuNC@DHLA was determined with gel electrophoresis to be smaller than 5 nm (Figure 3b), using bis(p-sulfonatophenyl)-phenylphosphine capped Au NPs of different size as standard. Hereby similar negative charge on the reference Au NPs and the Au NCs reported in this study was assumed.[46] These data suggest very small effective particle diameters in colloidal solution well below 5 nm. The size increment compared to the TEM results which refer to the diameter of only the inorganic Au core is attributed to the thickness of the organic capping of the particle surface with DHLA and adsorbed counterions. Due to their small size the AuNC@DHLA particles also showed excellent colloidal stability in buffer solution such as with 150 mM NaCl.

(Bio-)conjugation. Polyethylene glycol (PEG, 5 kDa) was chosen as the first example of a molecule to conjugate to the surface of AuNC@DHLA. PEG-coated particles are known for excellent biocompatibility, reduced nonspecific interaction with biological molecules and cells,[47,48] and increased coloidal stability in a salt-containing solution because of steric repulsion.[49−52] In previous studies[53,54] we have described that the more PEG molecules are attached to nanoparticles, the slower the PEGylated nanoparticles run with gel electrophoresis because of increased size of the conjugates. Attachment of single amino-terminated PEG molecules (methoxy-PEG-NH_2, $M_w \geq 5000$ g/mol) to nanoparticles using EDC chemistry can yield to distinctly shifted bands upon gel electrophoresis.[53] Here we demonstrate that PEG-NH_2 can also be covalently attach to fluorescent AuNC@DHLA particles *via* EDC, which forms an amine-reactive *O*-acylisourea intermediate with carboxyl groups and thus mediates amide formation with primary amines. The results shown in Figure 4 indicate that EDC-mediated attachment of PEG-NH_2 retards the band of the conjugates on the gel. At least one discrete retarded band exists which we ascribe to Au NCs with exactly one PEG attached per particle.[54] As the Au NCs are very small,

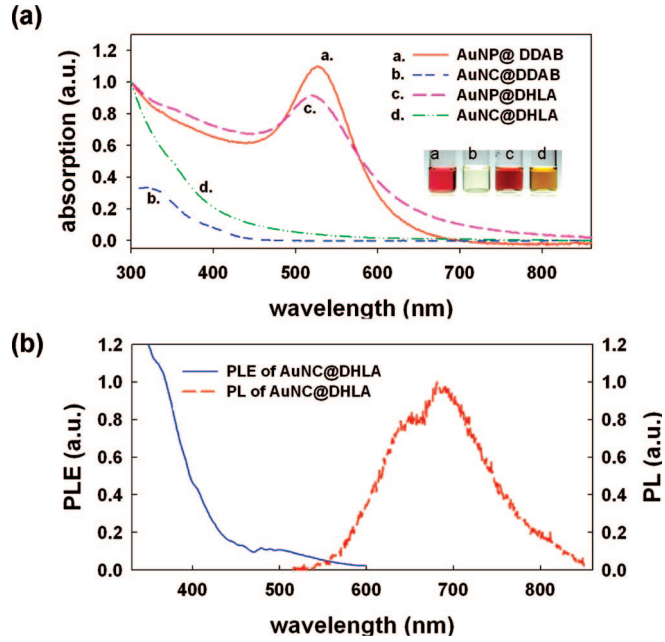

Figure 2. (a) UV−vis absorption spectra of the as-prepared gold nanoparticles (AuNP@DDAB), after etching (AuNC@DDAB), and after ligand exchange (AuNC@DHLA). The AuNP@DHLA sample was obtained by ligand exchange from the original AuNP@DDAB sample without etching step. Au samples with DDAB capping were dissolved in toluene, sample with DHLA capping in aqueous solution. (b) Photoluminescence (PL, dashed) and photoluminescence excitation spectra (PLE, solid) of AuNC@DHLA particles. For the PL spectrum, excitation at 490 nm was used. For the PLE spectrum, a fixed emission at 650 nm was used.

attachment of more PEG leads to complete retardation on the gel and conjugates with higher stoichiometry could not be resolved. PEGylation extraordinarily improved the stability of AuNC@DHLA in salt-containing buffer (1 M NaCl) as well as in acidic buffer (pH < 7). Similarly also biotin-PEG-amine could be attached to AuNC@DHLA following the same conjugation chemistry. In this case the unbound end of the PEG containing the biotin moiety is available as an anchor point for further bioconjugation, and the first discrete band can be ascribed to Au NCs with exactly one biotin functionality per NC. In a control experiment biotinylation of

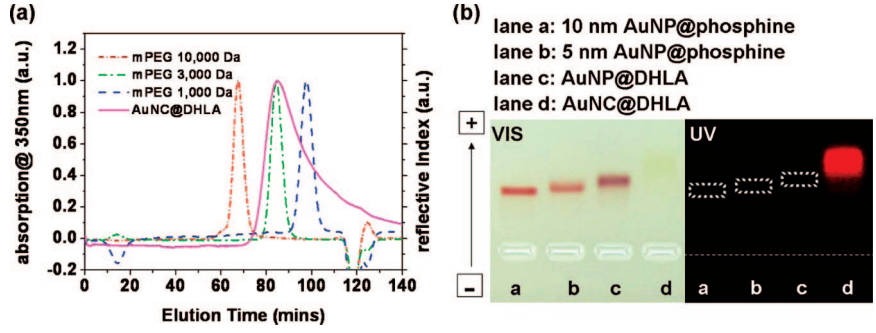

Figure 3. (a) Elution profile of size exclusion chromatography (Sephacryl S-200 gel) AuNC@DHLA particles *versus* PEG standards (1000, 3000, 10000 g/mol) as recorded *via* absorption or refractive index measurements. The PEG standards correspond to theoretically estimated diameters of 6.6, 3.4, and 1.8 nm. (b) Electrophoretic mobility of Au particles in 2% agarose gels (7.5 V/cm electric field, 20 min running time). Phosphine stabilized Au NPs of 10 and 5 nm core diameter were run in lanes a and b as control. In lanes c and d AuNP@DHLA and AuNC@DHLA solutions are run. The AuNP@DHLA corresponds to AuNP@DDAB after ligand exchange. Images were recorded at daylight (left) and under UV excitation (right).

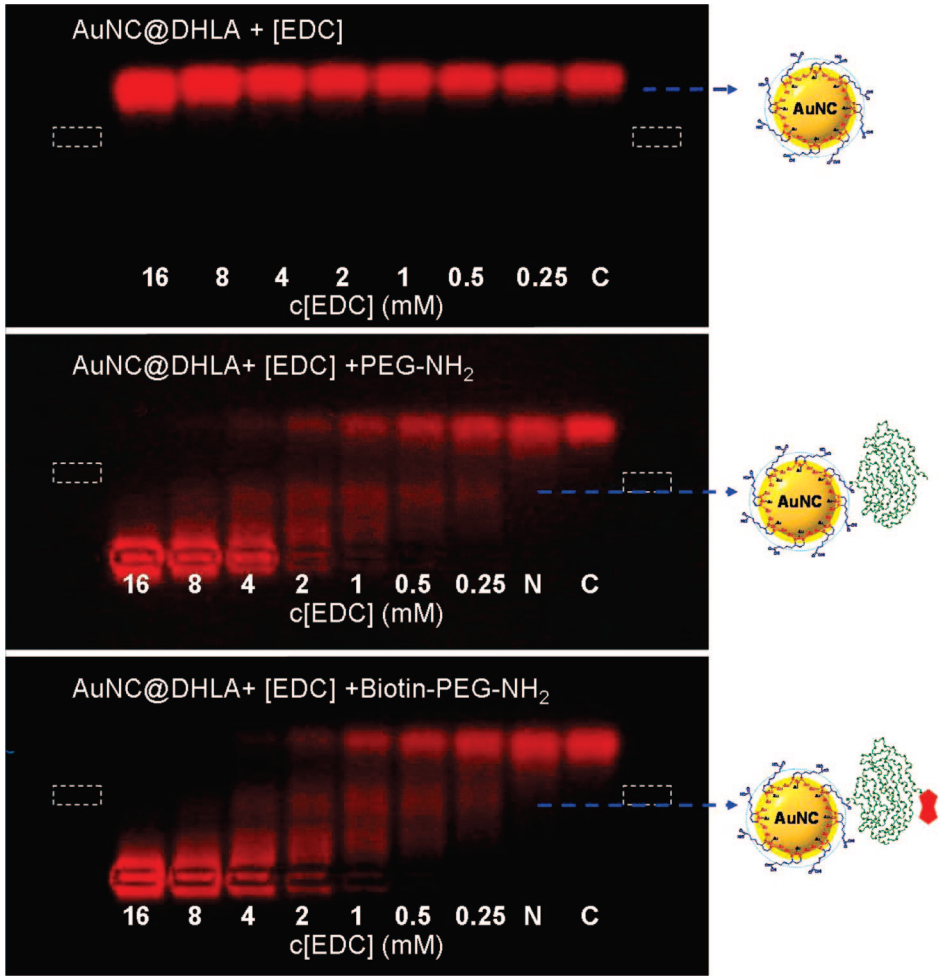

Figure 4. PEGylation and biotinylation of fluorescent Au nanoclusters (AuNC@DHLA) as probed with gel electrophoresis. The COOH groups present on the surface of AuNC@DHLA due to the DHLA capping allow for covalent linkage of NH_2-modified PEG molecules *via* EDC activation: (a) addition of EDC only to AuNC@DHLA serves as negative control without major effect in mobility; (b) addition of EDC under the presence of PEG−NH_2 retards the particle bands; (c) addition of EDC under the presence of biotin−PEG−NH_2 retards the particle bands. The terminal biotin groups are anchor points for further attachment of biological molecules *via* streptavidin. In both cases retardation is caused by linkage of PEG to the Au particles and the corresponding increment in size. The more the PEG is attached to AuNC@DHLA the larger the conjugates and thus the retardation become. We ascribe the first discrete band to Au particles with exactly one PEG linked per particle. The negative control (lane "N") represent AuNC@DHLA with PEG in the absence of EDC, and lane "C" is a control with AuNC@DHLA only.

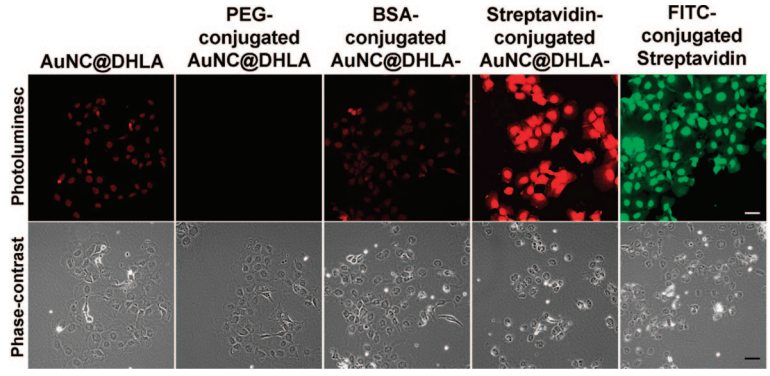

Figure 5. Labeling of endogenous biotin within human hepatoma cells ($HepG_2$) with fluorescent Au NCs conjugated to streptavidin (streptavidin-conjugated AuNC@DHLA). Three negative controls were used: unconjugated AuNC@DHLA, PEG-conjugated AuNC@DHLA, and BSA-conjugated AuNC@DHLA. Streptavidin-conjugated FITC served as positive control. All images were recorded with a 20× objective (PLAN NEOFLUAR) with a Zeiss confocal microscope. The fluorescence images were recorded with the following filter sets: AuNC@DHLA:LP 585 em/488 ex, FITC:LP 530/488 ex. The scale bars indicate 50 μm.

AuNC@DHLA was proven by cutting out the biotinylated Au NCs from gel, incubating them with streptavidin, and observation of the resulting increase in diameter due to biotin−streptavidin bond formation with gel electrophoresis (for date see the Supporting Information). PEGylation of AnNC@DHLA did not lead to reduction in photoluminescence intensity.

Avidin, a glycoprotein was chosen as second example for direct conjugation to AuNC@DHLA, as avidin−biotin technology has been widely used in biomedical research. Avidin molecules contain NH_2 groups and therefore can be conjugated to fluorescent AuNC@DHLA by EDC chemistry. Again attachment of avidin led to a reduction in mobility of the conjugates due to its high molecular weight of approximately 66 kDa (see Supporting Information for data). Similar results were obtained for streptavidin. In both cases conjugation of AuNC@DHLA did not lead to a reduction in particle photoluminescence.

Specific Labeling of Fixed Cells. Biotin, a vitamin essential for metabolism, is widely distributed in the body. Significant amounts of endogenous biotin have been detected in rat kidney, liver, and brain.[55] Probing the intracellular distribution of endogenous biotin within liver cells with streptavidin-conjugated AuNC@DHLA was therefore used as an example for confirming the functionality of streptavidin-conjugation. Human hepatoma cells ($HepG_2$) were fixed with 2% paraformaldehyde and stained with streptavidin-conjugated AuNC@DHLA. Unconjugated, PEG-conjugated, and BSA-conjugated AuNC@DHLA were used as negative control, and FITC-avidin was used as positive control (Figure 5). Bovine serum albumine (BSA) served hereby as control for a protein which does not specifically bind to biotin. How-

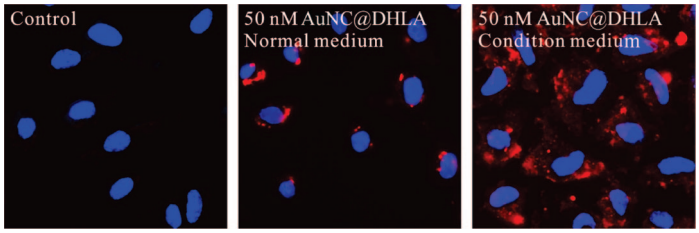

Figure 6. Nonspecific uptake of unconjugated fluorescent Au nanoclusters (AuNC@DHLA) by human aortic endothelial cells. Cell nuclei were stained with (Hochest 33258) to yield blue fluorescence. The red fluorescence corresponds to the Au NCs: (a) control without Au NCs; (b) serum-supplemented cell medium with 50 nM AuNC@DHLA added; (c) serum-free cell medium with 50 nM AuNC@DHLA added for 5 h.

ever, some red fluorescence can be observed in the labeling of the cells incubated with unconjugated and with BSA-conjugated Au NCs. In both cases this is referred to as nonspecific background. Conjugation of the Au NCs with PEG-reduced nonspecific binding was as expected, which can be seen in the very low red fluorescence intensity. Streptavidin-conjugated Au NCs on the other hand stained the biotin containing cells with high intensity. These results are in agreement with the positive control in which streptavidin-coated FITC was used, which is a common way to label the endogenous biotin.[55] The conclusion from *in situ* observation within liver cells was that the streptavidin-conjugated AuNC@DHLA can specifically label endogeneous biotin.

Nonspecific Uptake by Living Cells. In addition preliminary data indicate that fluorescent AuNC@DHLA without any modification did not cause any acute toxicity. Au NCs were nonspecifically incorporated by cells, as it is known also for colloidal quantum dots.[56] Uptake of unconjugated AuNC@DHLA was observed in living endothelial cells after around 5 h incubation (Figure 6). Here the uptake efficiency depended significantly on the culture medium, as incorporation was stronger in serum-free than in serum-supplemented medium.

CONCLUSIONS

In this report we describe the synthesis of water-soluble fluorescent gold nanoclusters capped with dihydrolipoic acid (DHLA). The resulting AuNC@DHLA particles have a quantum yield of around 1−3%, reduced photobleaching compared to organic fluorophores, and very good colloidal stability. AuNC@DHLA can be conjugated with EDC chemistry to biologically relevant molecules such as PEG, BSA, avidin, and streptavidin. Uptake of AuNC@DHLA by cells did not cause acute toxicity. By their small hydrodynamic diameter (<5 nm) and inert nature fluorescent Au NCs might become an interesting alternative to colloidal quantum dots, in particular for applications in which the size and biocompatibility of the label is critical. The weakest point so far remains the relatively low quantum yield. On the basis of the current report as well as on previous breakthrough findings[5,8,14,23,34,57] we believe that fluorescent gold nanoclusters have a great potential for applications to biomedical research to offer.

SYNTHESIS

Synthesis of Au NCs was based on precursor-induced Au NP etching. First 6-nm diameter gold NPs stabilized with didodecyldimethylammonium bromide (AuNP@DDAB) were synthesized in toluene *via* an established single-phase reaction[58] (experimental details can be found in the Supporting Information). The Au NPs isolated by methanol-induced agglomeration were then re-dissolved in toluene. The resulting red translucent NP solution showed the typical plasmon absorption peak at 520 nm, and transmission electron microscopy (TEM) analysis revealed a mean particle diameter of the inorganic Au core of 5.55 ± 0.68 nm. Subsequent further dropwise addition of gold precursor solution ($AuCl_3$ or $HAuCl_4$ in DDAB-toluene solution) caused a gradual loss of plasmon absorption until the solution turned colorless transparent (see Figure 1). TEM analysis of the transparent solution discovered the presence of small NCs with homogeneous size distribution (mean diameter 3.17 ± 0.35 nm as determined with TEM). This suggests that continuous addition of precursor started to etch the original nanoparticles of around 6 nm diameter (AuNP@DDAB) into smaller nanoclusters of around 3 nm diameter (AuNC@DDAB)[20,59] (for a set of time-dependent absorption spectra see the Supporting Information). As no change in solvent was involved in the etching procedure the Au NCs at this step still were dispersed in toluene. However, because for intended biological applications water-soluble Au NCs are required, a phase transfer to aqueous solution was carried out. For this purpose ligand exchange with reduced lipoic acid (DHLA, dihydrolipoic acid) was performed, a capping ligand which has already been successfully used for phase transfer.[60] Lipoic acid was freshly reduced by tetrabutylammonium borohydride (TBAB) with a molar ratio of lipoic acid to of TBAB = 4:1 and added to the AuNC@DDAB particles dispersed in toluene. This led to dark-brown particle agglomerates in the resulting mixture. Particles were precipitated by centrifugation, the toluene-based supernatant was discarded and the remaining particle precipitate could be dispersed in alkaline aqueous solution (pH 9) or methanol (basified by a small amount of alkaline buffer). Further purification was achieved by two runs of ultracentrifugation (110000 rpm) for removing excess DHLA, and the particle solution was concentrated with a centrifuge filter of 30 kDa MWCO (molecular weight cutoff), leading to a colloidally stable transparent solution of NCs without plasmon peak. Successful transfer from toluene to alkaline buffer solution suggests that the added DHLA had replaced the DDAB surfactants driven by the formation of gold-thiol bonds. TEM images showed that the resulting AuNC@DHLA particles were well-dispersed and had an average core diameter of 1.56 ± 0.3 nm. This demonstrates that the diameter of the Au NCs was further decreased during the ligand exchange procedure.

Acknowledgment. This project was supported by the National Science Council (NSC 96-2320-B-033; NSC 97-2627-B-033), the Ministry of Education from Taiwan, and in part by the Deutsche Forschungsgesellschaft (DFG, grant PA794/4-1) and the Bundesministerium für Bildung and Forschung (BMBF, grant 13N9192).

Supporting Information Available: Synthesis, size characterization, optical properties, bioconjugation, labeling of living and fixed cells. This material is available free of charge *via* the Internet at http://pubs.acs.org.

REFERENCES AND NOTES

1. Bigioni, T. P.; Whetten, R. L.; Dag, O. Near-Infrared Luminescence from Small Gold Nanocrystals. *J. Phys. Chem. B* **2000**, *104*, 6983–6986.
2. Huang, T.; Murray, R. W. Visible Luminescence of Water-Soluble Monolayer- Protected Gold Clusters. *J. Phys. Chem. B* **2001**, *105*, 12498–12502.
3. Peyser, L. A.; Vinson, A. E.; Bartko, A. P.; Dickson, R. M. Photoactivated Fluorescence from Individual Silver Nanoclusters. *Science* **2001**, *291*, 103–106.
4. Zheng, J.; Dickson, R. M. Individual Water-Soluble Dendrimer-Encapsulated Silver Nanodot Fluorescence. *J. Am. Chem. Soc.* **2002**, *124*, 13982–13983.
5. Link, S.; Beeby, A.; FitzGerald, S.; El-Sayed, M. A.; Schaaff, T. G.; Whetten, R. L. Visible to Infrared Luminescence from a 28-Atom Gold Cluster. *J. Phys. Chem. B* **2002**, *106*, 3410–3415.
6. Yang, Y.; Chen, S. Surface Manipulation of the Electronic Energy of Subnanometer-Sized Gold Clusters: An Electrochemical and Spectroscopic Investigation. *Nano Lett.* **2003**, *3*, 75–79.
7. Zheng, J.; Petty, J. T.; Dickson, R. M. High Quantum Yield Blue Emission from Water-Soluble Au-8 Nanodots. *J. Am. Chem. Soc.* **2003**, *125*, 7780–7781.
8. Negishi, Y.; Takasugi, Y.; Sato, S.; Yao, H.; Kimura, K.; Tsukuda, T. Magic-Numbered Au-N Clusters Protected by Glutathione Monolayers ($N = 18, 21, 25, 28, 32, 39$): Isolation and Spectroscopic Characterization. *J. Am. Chem. Soc.* **2004**, *126*, 6518–6519.
9. Schaaff, T. G.; Whetten, R. L. Giant Gold-Glutathione Cluster Compounds: Intense Optical Activity in Metal-Based Transitions. *J. Phys. Chem. B* **2000**, *104*, 2630–2641.
10. Garzon, I. L.; Reyes-Nava, J. A.; Rodriguez-Hernandez, J. I.; Sigal, I.; Beltran, M. R.; Michaelian, K. Chirality in Bare and Passivated Gold Nanoclusters. *Phys. Rev. B* **2002**, *66*, 073403-1–073403-4.
11. Gautier, C.; Bürgi, T. Chiral Inversion of Gold Nanoparticles. *J. Am. Chem. Soc.* **2008**, *130*, 7077–7084.
12. Roman-Velazquez, C. E.; Noguez, C.; Garzon, I. L. Circular Dichroism Simulated Spectra of Chiral Gold Nanoclusters: A Dipole Approximation. *J. Phys. Chem. B* **2003**, *107*, 12035–12038.
13. Crespo, P.; Litran, R.; Rojas, T. C.; Multigner, M.; de la Fuente, J. M.; Sanchez-Lopez, J. C.; Garcia, M. A.; Hernando, A.; Penades, S.; Fernandez, A. Permanent Magnetism, Magnetic Anisotropy, and Hysteresis of Thiol-Capped Gold Nanoparticles. *Phys. Rev. Lett.* **2004**, *93*, 087204-1–087204-4.
14. Chen, S.; Ingram, R. S.; Hostetler, M. J.; Pietron, J. J.; Murray, R. W.; Schaaff, T. G.; Khoury, J. T.; Alvarez, M. M.; Whetten, R. L. Gold Nanoelectrodes of Varied Size: Transition to Molecule-like Charging. *Science* **1998**, *280*, 2098–2101.
15. Hicks, J. F.; Templeton, A. C.; Chen, S. W.; Sheran, K. M.; Jasti, R.; Murray, R. W.; Debord, J.; Schaaf, T. G.; Whetten, R. L. The Monolayer Thickness Dependence of Quantized Double-Layer Capacitances of Monolayer-Protected Gold Clusters. *Anal. Chem.* **1999**, *71*, 3703–3711.
16. Hicks, J. F.; Miles, D. T.; Murray, R. W. Quantized Double-Layer Charging of Highly Monodisperse Metal Nanoparticles. *J. Am. Chem. Soc.* **2002**, *124*, 13322–13328.
17. Quinn, B. M.; Liljeroth, P.; Ruiz, V.; Laaksonen, T.; Kontturi, K. Electrochemical Resolution of 15 Oxidation States for Monolayer Protected Gold Nanoparticles. *J. Am. Chem. Soc.* **2003**, *125*, 6644–6645.
18. Lee, T. H.; Gonzalez, J. I.; Zheng, J.; Dickson, R. M. Single-Molecule Optoelectronics. *Acc. Chem. Res.* **2005**, *38*, 534–541.
19. Vosch, T.; Antoku, Y.; Hsiang, J. C.; Richards, C. I.; Gonzalez, J. I.; Dickson, R. M. Strongly Emissive Individual DNA-Encapsulated Ag Nanoclusters as Single-Molecule Fluorophores. *Proc. Natl. Acad. Sci. U.S.A.* **2007**, *104*, 12616–12621.
20. Huang, C. C.; Yang, Z.; Lee, K. H.; Chang, H. T. Synthesis of Highly Fluorescent Gold Nanoparticles for Sensing Mercury(II). *Angew. Chem., Int. Ed.* **2007**, *46*, 6824–6828.
21. Triulzi, R. C.; Micic, M.; Giordani, S.; Serry, M.; Chiou, W. A.; Leblanc, R. M. Immunoasssay Based on the Antibody-Conjugated Pamam-Dendrimer-Gold Quantum Dot Complex. *Chem. Commun.* **2006**, 5068–5070.
22. Huang, C. C.; Chiang, C. K.; Lin, Z. H.; Lee, K. H.; Chang, H. T. Bioconjugated Gold Nanodots and Nanoparticles for Protein Assays Based on Photoluminescence Quenching. *Anal. Chem.* **2008**, *80*, 1497–1504.
23. Zheng, J.; Zhang, C. W.; Dickson, R. M. Highly Fluorescent, Water-Soluble, Size-Tunable Gold Quantum Dots. *Phys. Rev. Lett.* **2004**, *93*, 077402-1–077402-4.
24. Link, S.; El-Sayed, M. A. Optical Properties and Ultrafast Dynamics of Metallic Nanocrystals. *Annu. Rev. Phys. Chem.* **2003**, *54*, 331–66.
25. Alvarez, M. M.; Khoury, J. T.; Schaaff, T. G.; Shafigullin, M. N.; Vezmar, I.; Whetten, R. L. Optical Absorption Spectra of Nanocrystal Gold Molecules. *J. Phys. Chem. B* **1997**, *101*, 3706–3712.
26. Schaaff, T. G.; Shafigullin, M. N.; Khoury, J. T.; Vezmar, I.; Whetten, R. L.; Cullen, W. G.; First, P. N.; GutierrezWing, C.; Ascensio, J.; JoseYacaman, M. J. Isolation of Smaller Nanocrystal Au Molecules: Robust Quantum Effects in Optical Spectra. *J. Phys. Chem. B* **1997**, *101*, 7885–7891.
27. Hostetler, M. J.; Wingate, J. E.; Zhong, C. J.; Harris, J. E.; Vachet, R. W.; Clark, M. R.; Londono, J. D.; Green, S. J.; Stokes, J. J.; Wignall, G. D.; *et al* Alkanethiolate Gold Cluster Molecules with Core Diameters from 1.5 to 5.2 Nm: Core and Monolayer Properties as a Function of Core Size. *Langmuir* **1998**, *14*, 17–30.
28. Schaeffer, N.; Tan, B.; Dickinson, C.; Rosseinsky, M. J.; Laromaine, A.; McComb, D. W.; Stevens, M. M.; Wang, Y.; Petit, L.; Barentin, C.; *et al* Fluorescent or Not? Size-Dependent Fluorescence Switching for Polymer-Stabilized Gold Clusters in the 1.1−1.7 nm Size Range. *Chem. Comm.* **2008**, 3986–3988.
29. Apell, P.; Monreal, R.; Lundqvist, S. Photoluminescence of Noble Metals. *Phys. Scr.* **1988**, *38*, 174–179.
30. Lee, D.; Donkers, R. L.; Wang, G. L.; Harper, A. S.; Murray, R. W. Electrochemistry and Optical Absorbance and Luminescence of Molecule-like Au-38 Nanoparticles. *J. Am. Chem. Soc.* **2004**, *126*, 6193–6199.
31. Lin, Z. Y.; Kanters, R. P. F.; Mingos, D. M. P. Closed-Shell Electronic Requirements for Condensed Clusters of the Group-11 Elements. *Inorg. Chem.* **1991**, *30*, 91–95.
32. Fedrigo, S.; Harbich, W.; Buttet, J. Optical-Response of Ag2, Ag3, Au2, and Au3 in Argon Matrices. *J. Chem. Phys.* **1993**, *99*, 5712–5717.
33. Konig, L.; Rabin, I.; Schulze, W.; Ertl, G. Chemiluminescence in the Agglomeration of Metal Clusters. *Science* **1996**, *274*, 1353–1355.
34. Wilcoxon, J. P.; Martin, J. E.; Parsapour, F.; Wiedenman, B.; Kelley, D. F. Photoluminescence from Nanosize Gold Clusters. *J. Chem. Phys.* **1998**, *108*, 9137–9143.
35. Mooradian, A. Photoluminescence of Metals. *Phys. Rev. Lett.* **1969**, *22*, 185–187.
36. Boyd, G. T.; Yu, Z. H.; Shen, Y. R. Photoinduced Luminescence from the Noble-Metals and Its Enhancement on Roughened Surfaces. *Phys. Rev. B* **1986**, *33*, 7923–7936.
37. Sperling, R. A.; Gil, P. R.; Zhang, F.; Zanella, M.; Parak, W. J. Biological Applications of Gold Nanoparticles. *Chem. Soc. Rev.* **2008**, *37*, 1896–1908.
38. Alivisatos, A. P. Semiconductor Clusters, Nanocrystals, and Quantum Dots. *Science* **1996**, *271*, 933–937.
39. Kirchner, C.; Liedl, T.; Kudera, S.; Pellegrino, T.; Javier, A. M.; Gaub, H. E.; Stolzle, S.; Fertig, N.; Parak, W. J. Cytotoxicity of Colloidal Cdse and Cdse/Zns Nanoparticles. *Nano Lett.* **2005**, *5*, 331–338.

40. Pan, Y.; Neuss, S.; Leifert, A.; Fischler, M.; Wen, F.; Simon, U.; Schmid, G.; Brandau, W.; Jahnen-Dechent, W. Size-Dependent Cytotoxicity of Gold Nanoparticles. *Small* **2007**, *3*, 1941–1949.
41. Negishi, Y.; Tsukuda, T. Visible Photoluminescence from Nearly Monodispersed Au-12 Clusters Protected by Meso-2,3-Dimercaptosuccinic Acid. *Chem. Phys. Lett.* **2004**, *383*, 161–165.
42. Negishi, Y.; Nobusada, K.; Tsukuda, T. Glutathione-Protected Gold Clusters Revisited: Bridging the Gap between Gold(I)-Thiolate Complexes and Thiolate-Protected Gold Nanocrystals. *J. Am. Chem. Soc.* **2005**, *127*, 5261–5270.
43. Wang, G. L.; Huang, T.; Murray, R. W.; Menard, L.; Nuzzo, R. G. Near-Ir Luminescence of Monolayer-Protected Metal Clusters. *J. Am. Chem. Soc.* **2005**, *127*, 812–813.
44. Cha, S. H.; Kim, J. U.; Kim, K. H.; Lee, J. C. Preparation and Photoluminescent Properties of Gold(I)-Alkanethiolate Complexes Having Highly Ordered Supramolecular Structures. *Chem. Mater.* **2007**, *19*, 6297–6303.
45. Scolari, M.; Vogel, E. K.; Awh, E. Perceptual Expertise Enhances the Resolution but Not the Number of Representations in Working Memory. *Psychonom. Bull. Rev.* **2008**, *15*, 215–222.
46. Sperling, R. A.; Liedl, T.; Duhr, S.; Kudera, S.; Zanella, M.; Lin, C.-A. J.; Chang, W. H.; Braun, D.; Parak, W. J. Size Determination of (Bio-)conjugated Water-Soluble Colloidal Nanoparticles—A Comparison of Different Techniques. *J. Phys. Chem. C* **2007**, *111*, 11552–11559.
47. Ballou, B.; Lagerholm, B. C.; Ernst, L. A.; Bruchez, M. P.; Waggoner, A. S. Noninvasive Imaging of Quantum Dots in Mice. *Bioconjugate Chem.* **2004**, *15*, 79–86.
48. Bentzen, E. L.; Tomlinson, I. D.; Mason, J.; Gresch, P.; Warnement, M. R.; Wright, D.; Sanders-Bush, E.; Blakely, R.; Rosenthal, S. J. Surface Modification to Reduce Nonspecific Binding of Quantum Dots in Live Cell Assays. *Bioconjugate Chem.* **2005**, *16*, 1488–1494.
49. Dubertret, B.; Skourides, P.; Norris, D. J.; Noireaux, V.; Brivanlou, A. H.; Libchaber, A. In Vivo Imaging of Quantum Dots Encapsulated in Phospholipid Micelles. *Science* **2002**, *298*, 1759–1762.
50. Parak, W. J.; Gerion, D.; Zanchet, D.; Woerz, A. S.; Pellegrino, T.; Micheel, C.; Williams, S. C.; Seitz, M.; Bruehl, R. E.; Bryant, Z.; et al. Conjugation of DNA to Silanized Colloidal Semiconductor Nanocrystaline Quantum Dots. *Chem. Mater.* **2002**, *14*, 2113–2119.
51. Nikolic, M. S.; Krack, M.; Aleksandrovic, V.; Kornowski, A.; Forster, S.; Weller, H. Tailor-Made Ligands for Biocompatible Nanoparticles. *Angew. Chem., Int. Ed.* **2006**, *45*, 6577–6580.
52. Mei, B. C.; Susumu, K.; Medintz, I. L.; Delehanty, J. B.; Mountziaris, T. J.; Mattoussi, H. Modular Poly(Ethylene Glycol) Ligands for Biocompatible Semiconductor and Gold Nanocrystals with Extended Ph and Ionic Stability. *J. Mater. Chem.* **2008**, *18*, 4949–4958.
53. Sperling, R. A.; Pellegrino, T.; Li, J. K.; Chang, W. H.; Parak, W. J. Electrophoretic Separation of Nanoparticles with a Discrete Number of Functional Groups. *Adv. Funct. Mater.* **2006**, *16*, 943–948.
54. Lin, C. A. J.; Sperling, R. A.; Li, J. K.; Yang, T. Y.; Li, P. Y.; Zanella, M.; Chang, W. H.; Parak, W. G. J. Design of an Amphiphilic Polymer for Nanoparticle Coating and Functionalization. *Small* **2008**, *4*, 334–341.
55. Wang, H.; Pevsner, J. Detection of Endogenous Biotin in Various Tissues: Novel Functions in the Hippocampus and Implications for Its Use in Avidin-Biotin Technology. *Cell Tissue Res.* **1999**, *296*, 511–516.
56. Parak, W.; Boudreau, R.; Le Gros, M.; Gerion, D.; Zanchet, D.; Micheel, C.; Williams, S.; Alivisatos, A.; Larabell, C. Cell Motility and Metastatic Potential Studies Based on Quantum Dot Imaging of Phagokinetic Tracks. *Adv. Mater.* **2002**, *14*, 882–885.
57. Jadzinsky, P. D.; Calero, G.; Ackerson, C. J.; Bushnell, D. A.; Kornberg, R. D. Structure of a Thiol Monolayer-Protected Gold Nanoparticle at 1.1 Angstrom Resolution. *Science* **2007**, *318*, 430–433.
58. Jana, N. R.; Peng, X. G. Single-Phase and Gram-Scale Routes toward Nearly Monodisperse Au and Other Noble Metal Nanocrystals. *J. Am. Chem. Soc.* **2003**, *125*, 14280–14281.
59. Kruger, D.; Fuchs, H.; Rousseau, R.; Marx, D.; Parrinello, M. Interaction of Short-Chain Alkane Thiols and Thiolates with Small Gold Clusters: Adsorption Structures and Energetics. *J. Chem. Phys.* **2001**, *115*, 4776–4786.
60. Mattoussi, H.; Mauro, J.; Goldman, E.; Anderson, G.; Sundar, V.; Mikulec, F.; Bawendi, M. Self-Assembly of Cdse-Zns Quantum Dot Bioconjugates Using an Engineered Recombinant Protein. *J. Am. Chem. Soc.* **2000**, *122*, 12142–12150.